Dipolar Structures in Colloidal Dispersions of PbSe and CdSe Quantum Dots

Mark Klokkenburg,[†,‡] Arjan J. Houtepen,[*,†,§] Rolf Koole,[§] Julius W. J. de Folter,[§] Ben H. Erné,[‡] Ernst van Faassen,[∥] and Daniël Vanmaekelbergh[§]

Van 't Hoff Laboratory for Physical and Colloid Chemistry, Faculty of Science, Utrecht University, Padualaan 8, 3584 CH Utrecht, The Netherlands, Condensed Matter and Interfaces, Faculty of Science, Utrecht University, Princetonplein 1, 3508 TH Utrecht, The Netherlands, and Surfaces, Interfaces and Devices, Faculty of Science, Utrecht University, 3508 TA Utrecht, The Netherlands

ABSTRACT

We show by cryogenic transmission electron microscopy that PbSe and CdSe nanocrystals of various shapes in a liquid colloidal dispersion self-assemble into equilibrium structures that have a pronounced dipolar character, to an extent that depends on particle concentration and size. Analyzing the cluster-size distributions with a one-dimensional (1D) aggregation model yields a dipolar pair attraction of 8–10 $k_B T$ at room temperature. This accounts for the long-range alignment of the crystal planes of individual nanocrystals in self-assembled superstructures and for anisotropic nanostructures grown via oriented attachment.

Anisotropic features in self-assembled structures of semiconductor nanocrystals (NCs) point to the presence of a directive force on the particles.[1−4] An example is the growth of single-crystalline nanowires from PbSe NCs, which indicates that the particles attach to each other in a precise orientation.[3] The origin of the underlying directive force observed for various types of nanocrystals is still under debate. CdSe has a wurtzite crystal structure that can, in principle, account for a dipole moment.[5,6] In contrast, the rock-salt lattice of PbSe and the zinc-blende lattice of, e.g., ZnSe, are centrosymmetric and cannot explain dipole moments in nanocrystals of these materials.[7] It has been suggested that nanocrystal dipole moments result from the distribution of differently terminated polar crystal facets[3] or from charged surface states.[7]

Dipolar coupling was also suggested to play a role in the self-assembly of semiconductor NCs into ordered films.[4,8] However, the unknown strength of the proposed dipolar attraction makes it difficult to evaluate its importance compared to capillary drying effects. Very recently, Talapin et al. presented calculations on the effect of a NC dipole moment on the structure of self-assembled supercrystals of,

among other things, PbSe nanocrystals.[9] In spite of the fact that the strength of the dipolar interaction is the most important parameter in such calculations, it has up to now not been experimentally determined for that system. Moreover, the model proposed by Cho et al. for the origin of the dipole moment in NCs with a rock-salt lattice[3] has not been tested experimentally. Whatever its origin, a dipolar interaction may have an important impact on the ordering and optoelectrical properties of assemblies of the NCs. Here we provide independent experimental evidence for the presence of a directive force between semiconductor NCs by demonstrating that it leads to anisotropic aggregates in liquid colloidal dispersions of the particles.

In previous studies, the dipole moment of NCs such as CdSe and ZnSe has been determined through the dielectric response from rotation of single particles that are exposed to an oscillating electric field.[5,7,10] However, the more relevant parameter to describe the interaction between NCs in dispersion or in assemblies is their pair interaction rather than a dipole moment. The pair interaction may contain higher multipole moments when the particles are at close distance and may be significantly larger than the dipole interaction alone.

We present the first determination of the total pair interaction between semiconductor NCs in dispersion. Our novel approach to quantify dipolar attractions between NCs is by image analysis of equilibrium structures in colloidal dispersions of sterically stabilized particles visualized by cryogenic transmission electron microscopy (cryo-TEM).[11−14]

* Corresponding author. E-mail: a.j.houtepen@phys.uu.nl. Current address: Optoelectronic Materials, Faculty of Applied Sciences, Delft University of Technology, Julianalaan 136, 2628 BL Delft, The Netherlands.
† M.K. and A.J.H. have contributed equally to this work.
‡ Van 't Hoff Laboratory for Physical and Colloid Chemistry, Faculty of Science, Utrecht University.
§ Condensed Matter and Interfaces, Faculty of Science, Utrecht University.
∥ Surfaces, Interfaces and Devices, Faculty of Science, Utrecht University.

Table 1. Shape, Composition, Average Particle Size d, Surface Fraction θ, and Determined Pair Interaction V (See Text) of Systems A−F

code	shape	composition	TEM diameter d (nm)	surface fraction θ	V (k_BT)
A	sphere	PbSe	6.8 ± 0.3	0.01	-8.0 ± 1
B	sphere	PbSe	6.8 ± 0.3	0.06	-8.0 ± 1
C	sphere	PbSe	6.8 ± 0.3	0.16	-8.0 ± 1
D	cube	PbSe	11.1 ± 0.6	0.12	-9.0 ± 2
E	star	PbSe	12.8 ± 1.6	0.02	-10.0 ± 2
F	sphere	CbSe	5.9 ± 0.7	0.09	-9.0 ± 2

With this technique, we present in situ images of one-dimensional (1D) dipolar equilibrium nanostructures in thin (two-dimensional, 2D) vitrified films of PbSe and CdSe NC dispersions in decalin. Colloidal dispersions of PbSe and CdSe NCs are studied as a function of concentration and particle shape. We determine the interaction strength based on quantitative analysis of the imaged structures on the single-particle level.[15,16] The only prerequisite is that thermodynamic equilibrium prevails, which we show to be the case by investigating dispersions of different concentrations.

Colloidal PbSe and CdSe dispersions in decalin (A−F) were prepared by methods described previously[4,17] in which the size and the shape of the particles could be tuned. Table 1 lists the average particle diameters (d) determined by TEM, the particle concentration expressed in surface fractions θ ($= N_TA_p/A_I$, where N_T is the total number of particles in the images, A_p is the cross-sectional area of one particle, and A_I is the total area of all images) and the pair interaction V (see below). Cryo-TEM images were obtained by preparing a vitrified film of dispersion on grids with holey carbon film (R2/2 Quantifoil Micro Tools, Jena, Germany). A droplet of dispersion was placed onto the holey carbon grid, and excess solution was removed automatically with a vitrobot.[11,12] In this way, a free-standing liquid film was produced in the grid holes (diameter 2 μm) with a thickness of the order of one nanoparticle diameter. Thermal motion of the particles was arrested by plunging the film into liquid nitrogen.[18] The homogeneous gray background in Figure 1 demonstrates that the solvent is vitrified because crystallization would lead to strong scattering of the electron beam and, consequently, to loss of image resolution. While still in liquid nitrogen, the grids were placed into a specially devised cryoholder that could be mounted in the microscope. The presented CCD images were taken on a Philips Tecnai 12 TEM operating at 120 kV. Particle positions were tracked in 2D snapshots using image analysis software.[19] For all systems, at least six images were analyzed containing altogether more than 600 particles.

Panels A−C in Figure 1 present cryo-TEM snapshots obtained for dispersions A−C that contain spherical PbSe nanocrystals (see Table 1). The images clearly demonstrate the presence of single nanocrystals as well as straight and branched chains of particles in the liquid film and manifest the one-dimensional character of the structures. The snapshots in A−C correspond to different particle concentrations. The sample in A was prepared by diluting the sample in

panel C. We remark that the sample in panel B was prepared in a separate synthesis. This shows that the observed linear aggregation is a reproducible property of PbSe NC dispersions. The imaged structures strongly resemble the magnetic dipolar structures that have been observed recently in colloidal iron and magnetite dispersions.[13,14]

As a first quantification of the imaged dipolar structures, we calculated the radial distribution function $g(r)$, defined as:

$$g(\mathbf{r}) = \frac{1}{\rho} \left\langle \sum_{j \neq i} \delta(\mathbf{r}_i - \mathbf{r}_j - \mathbf{r}) \right\rangle_i \quad (1)$$

where ρ is the average number density, δ represents a delta function, $\mathbf{r}$ is the position vector, and the indices i and j run over all particles.[20]

The radial distribution function $g(r)$ for system A is shown in Figure 2a. The data show two peaks at $r = 9$ and 18 nm, indicating the predominance of linear aggregation. Furthermore, the position of the first maximum at 9 nm implies an "effective" interparticle separation r_{ip} of approximately 2.2 nm. This value is close to the length of a single oleic acid molecule and, therefore, suggests the presence of only a single layer between two neighboring particle surfaces.

The structures partially dissociate when the system is diluted (C → A), in line with our hypothesis that thermodynamic equilibrium exists between the structures of different lengths. To examine the equilibrium in more detail, we calculate the number of nearest neighbors per particle (Figure 2b). We define a neighbor as being located within a center-to-center distance of $d_c = 1.35\Delta$, where Δ is the mean center-to-center distance determined from the first maximum in $g(r)$. The calculations were not affected by the choice of the cutoff distance in the range $1.0-1.5\Delta$. For system C, the distribution peaks at 2 nearest neighbors, signaling the one-dimensional character of the structures. Note that coordination numbers larger than 2 indicate branching points. When system C is diluted by a factor of 16, the probability distribution shifts to 1 and the number of branching points decreases significantly, confirming the dissociation of the clusters.

The cluster-size distribution of these systems decays with increasing number of particles in a cluster, as is depicted in Figure 3a. We define a cluster as having one end particle that serves as a starting point; all the nearest neighbors of this particle are assigned to be part of this cluster, including their nearest neighbors, etc., until no new neighbors are detected. The average cluster size decreases from 4.5 in system C to 2 particles for system A, in line with a dynamic equilibrium. We now apply a one-dimensional aggregation model that we previously introduced to describe dipolar chain lengths in colloidal dispersions of magnetic nanoparticles.[21] This model only takes into account the effective nearest neighbor interaction V and gives the following relation between the concentrations of dipolar chains of different lengths q:
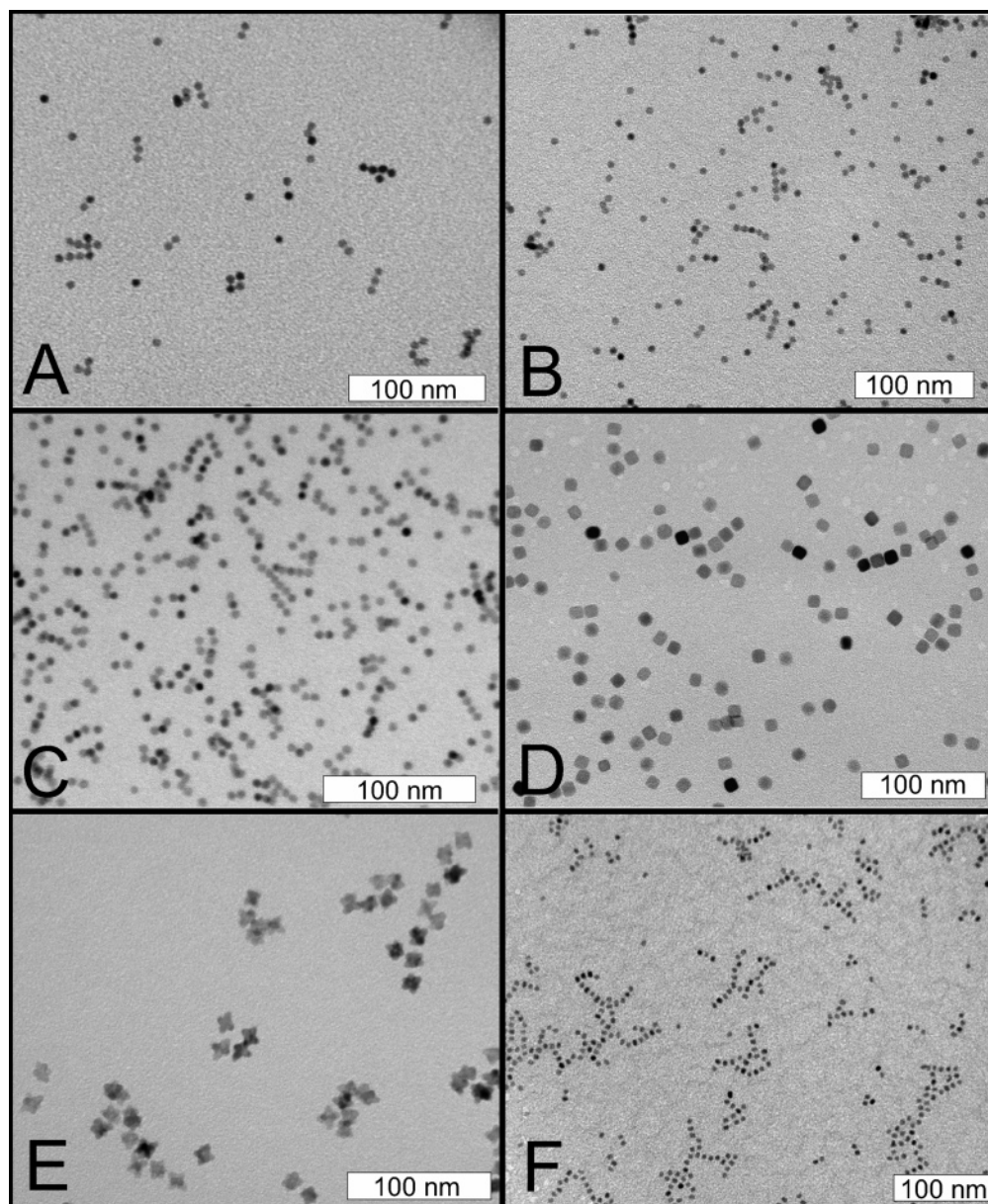
$$x_q = x_1^q \exp(-(q - 1)V) \quad (2)$$

Figure 1. Typical in situ cryo-TEM images of vitrified colloidal dispersions of PbSe (A−E) and CdSe (F) NCs. The surface fractions and chemical compositions are listed in Table 1. Anisotropic structures can be observed in all the images and clearly indicate the presence of a dipole moment, irrespective of particle shape or chemical composition.

where x_1 is the surface mole fraction of single particles and V is scaled to the thermal energy.[22,23] A fit to the initial decay (see inset Figure 3a) yields a value for V of -8 ± 1 and similar values for systems B and C. Beyond 3−4 particles in a cluster, a more detailed description is required that takes into account chain curvature. We conclude that the PbSe nanoparticles have a dipolar attraction of $-8 \pm 1 \, k_BT$ (room temperature) at minimal contact.

Figure 3b shows the average coordination number per cluster as a function of the cluster size for system A. The coordination number increases with increasing cluster size. Already at a cluster size of 4, the average coordination number reaches 2. Because a coordination number of 2 is only expected in the limit of infinite chains, this suggests deviations from linearity, for instance, the square or triangular structures of a few particles.

The effect of the particle shape is demonstrated in panels D and E in Figure 1. The particle shape is changed from spherical to cubic (panel D) upon increasing the nanocrystal size,[24] or to starlike by adding a small amount of acetic acid to the reaction mixture (panel E).[4] Interestingly, both the cubes and the stars exhibit similar linear structures as observed for the PbSe spheres. CdSe yields qualitatively similar pictures of particles that self-assemble into predominantly one-dimensional structures, although the aggregates appear more flexible than with PbSe, as is revealed by wormlike structures (panel F).

The directional interaction of NCs observed in cryo-TEM of colloidal dispersions directly affects the orientation of the NCs in 2D hexagonal self-assembled layers. Figure 4A shows a monolayer of spherical PbSe nanocrystals that form a nearly defect-free and single-crystalline area over several μm^2. The
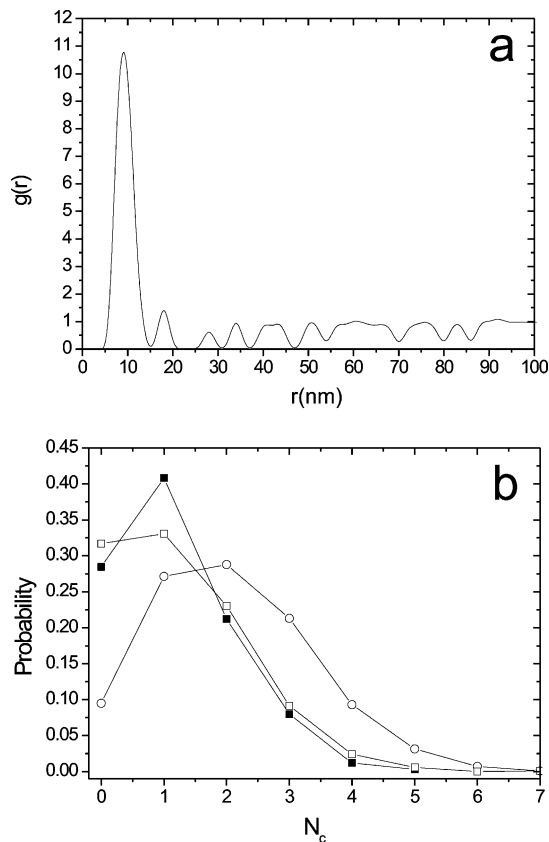
Figure 2. (a) Radial distribution function $g(r)$ obtained from the cryogenic 2D images for system A. (b) Histograms of the coordination number N_c probability of a particle in system A ($\blacksquare$), B ($\square$), and C ($\bigcirc$). Note that the coordination number probability of C peaks at $N_c = 2$, indicating predominantly linear structures.

Figure 3. (a) Cluster-size distribution of system A. The inset shows a fit to the data according to eq 2. Note that the relevant thermodynamic measure for concentration in this model is surface mole fraction.[22,23] (b) Average coordination number per cluster as a function of the cluster size for system A. The line through the data points is a guide to the eye.

Fourier transform of such a monolayer indicates the hexagonal symmetry with an average distance of 9.0 nm (panel B), in good agreement with the position of the first maximum in the radial distribution function (at 9 nm for the same batch of NCs, see Figure 2a). Panel C is a wide-angle electron diffraction (WAED) pattern of a 0.8 μm^2 subsection of the monolayer in panel A. In WAED, the diffraction is probed at angles corresponding to Bragg diffraction at atomic distances. This implies that WAED is sensitive to the crystal structure within the PbSe NCs and that it probes the crystal planes perpendicular to the electron beam. The occurrence of discrete peaks instead of rings in the WAED image demonstrates atomic alignment between the nanocrystals. We remark here that our observations differ from those of Talapin et al.[9] in that we have exclusively observed atomic alignment with the $\langle 111 \rangle$ crystal axis of the PbSe NCs toward the substrate (as six equidistant peaks are observed), whereas they have observed atomic alignment with the $\langle 100 \rangle$ axis toward the substrate. The substrates were similar carbon-coated polymer TEM grids for their and our experiments. The atomic alignment of the spherical NCs is also illustrated in panel D of Figure 4. It shows a TEM image of a 3D supercrystal of spherical nanocrystals with a 7.7 nm diameter, which self-assembled in a slightly destabilized dispersion. The inset is a WAED pattern of one of these supercrystals clearly showing a strong alignment of the atomic lattices of the individual NCs. Such atomic alignment can be induced
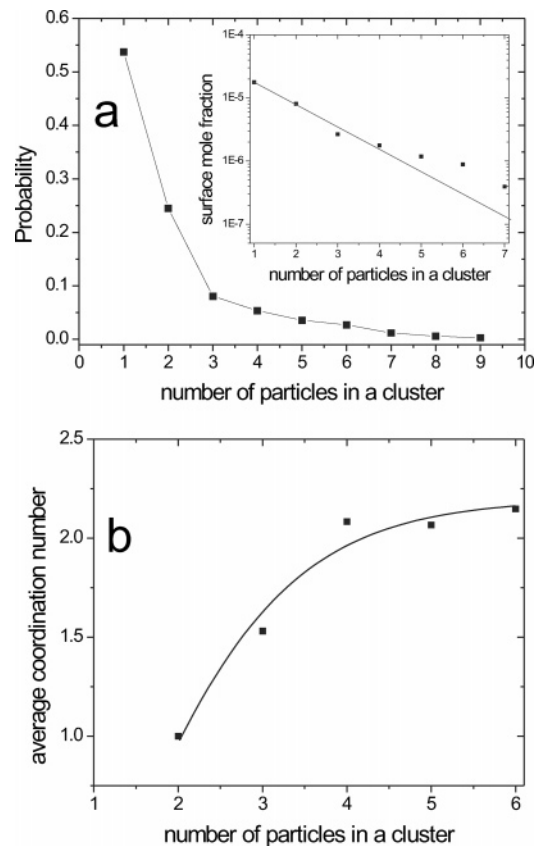
by the shape of the nanocrystals. For example, cubic nanocrystals exhibit cubic packing if two {100} facets face one another. However, the nanocrystals in Figure 4 are close to spherical and therefore it is likely that the atomic alignment is caused by dipolar interactions between the nanocrystals.

The presence of an electric dipole moment in nanocrystals with a centrosymmetric crystal structure (e.g., zinc-blende, rock-salt) can be partially explained by a theoretical model that ascribes the origin of the dipoles to differently charged facets.[3,7] The largest effect is expected from polar facets, such as the {111} facets in PbSe. Assuming an equal number of partially negatively charged (Se terminated) and positively charged (Pb terminated) {111} facets with a random geometrical distribution. Cho et al. have calculated that 90% of the NCs have a dipole moment.[3] A dipole moment along the $\langle 100 \rangle$ axis is the most frequent and, in addition, the strongest. Although this simple model neglects the influence of capping molecules, surface reconstructions, and the free-energy cost for the creation of a dipole, it has been used to explain various structures formed by oriented attachment of PbSe nanocrystals.[3,4] In the above model, the size of the dipole moment is determined by the total surface of the {111} facets. This should be the largest for the star-shaped nanocrystals, the smallest for the cubic nanocrystals (zero for perfect cubes) and intermediate for quasispherical nanocrystals. The cryo-TEM images indicate that both the cubes
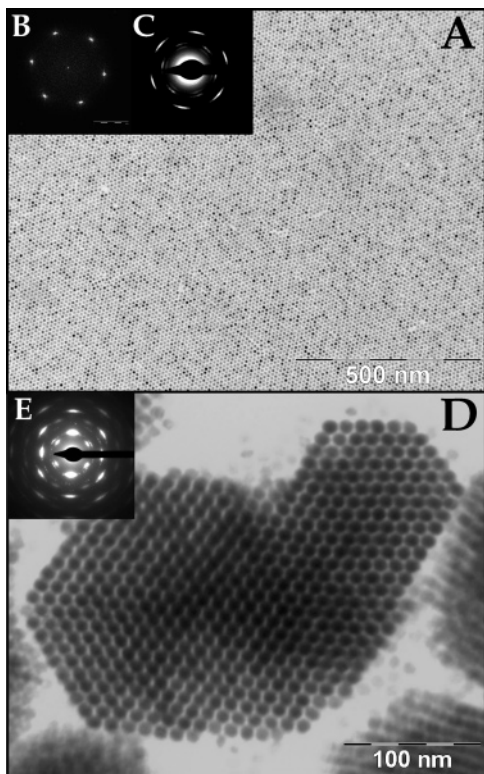
Figure 4. (A) Typical TEM image showing hexagonal monolayers of quasispherical PbSe nanocrystal of 6.8 ± 0.3 nm. (B) Fourier transform of image A showing the hexagonal symmetry and long-range order. The scale bar is 0.1 nm^{-1}. (C) WAED image of a 0.8 μm^2 subsection of the monolayer in A. (D) Typical TEM image showing a three-dimensional supercrystal formed by quasispherical PbSe nanocrystals of 7.7 nm. (E) WAED pattern on one super-crystal, clearly illustrating atomic alignment.

and the stars exhibit chain formation with a pronounced linear character. The extent to which these different systems form anisotropic structures is similar, including topological features as curvature etc. In light of the model by Cho et al., this means that the cubes still have a significant amount of {111} facets.

The analysis of the particle distributions in cryo-TEM yields the pair interactions that are listed in Table 1. Although this is the most important parameter to describe the interaction between the NCs, we will try to estimate the corresponding dipole moment in order to compare this value to other values from the literature.[5−7] The magnitude of the dipole moment determined from the pair interaction depends on the charge distribution that gives rise to this dipole moment. The dipole moment is usually obtained using the point-dipole approximation. The pair interaction V between two identical point dipoles in a head-to-tail configuration is given by[22]

$$V = \frac{-2\mu^2}{4\pi\epsilon\epsilon_0\Delta^3} \qquad (3)$$

where the distance Δ between the dipoles is equal to the mean center-to-center distance. It was noted recently by Talapin et al.[9] that this approximation should not be valid

for nanocrystals as the length of the dipoles (i.e., the NC diameter d) exceeds the interparticle distances. Instead, these authors chose to describe the dipole by point charges that are symmetrically placed on opposite sides of the NC. In this case, the interaction is given by

$$V = \frac{-q^2}{4\pi\epsilon\epsilon_0(\Delta - d)} + \frac{2q^2}{4\pi\epsilon\epsilon_0\Delta} + \frac{-q^2}{4\pi\epsilon\epsilon_0(\Delta + d)} =$$

$$\frac{-2\mu^2}{4\pi\epsilon\epsilon_0\Delta(\Delta^2 - d^2)} \qquad (4)$$

For systems A-C, with a pair interaction of $-8\ k_BT$, eq 3 yields a screened dipole moment of $\mu = 514$ D, while eq 4 gives $\mu = 337$ D (equivalent to $q \approx 1e$).[25] The point-dipole approximation appears to overestimate the effective dipole moment. However, eq 3 is in fact correct for a homogeneous spherical surface-charge distribution with positive and negative hemispheres on opposite sides of the nanocrystal because, from outside the NC, this potential is indistinguishable from a point dipole. The above-mentioned point-dipole and point-charge approximations are limiting cases of the possible charge distribution, with the charge completely spread out over the surface or condensed into two points, respectively. Any real surface-charge distribution will yield a dipole moment that is intermediate between the values obtained by eqs 3 and 4.

Irrespective of the approximation used, the dipole moments that we obtain are significantly larger than quantum-dot dipole moments that have been reported previously. The dipole moment we obtained for 5.9 nm CdSe nanoparticles (system F) is between 412 and 545 D (using eqs 4 and 3, respectively). In the past decade, several experiments have been described in the literature in which the response of CdSe dispersions was measured using electrical impedance spectroscopy[5,7,10] or transient birefringence measurements.[6] Both techniques rely the rotation of the dipolar particles in an external oscillating electric field. These measurements indicated the presence of an permanent (screened) electric dipole moment of 100 D for CdSe NCs with a 5.6 nm diameter.[7] Assuming a 3.1 nm interparticle separation (from our own measurements on CdSe NCs), eq 4 yields an upper estimate of $\sim-0.6\ k_BT$ at room temperature for the interparticle interaction if the dipole moment is 100 D. This interaction is too small to account for the anisotropic nanocrystals grown via oriented attachment.[1,3,4]

As is demonstrated by Figure 1, for strong dipolar interactions, large aggregates are expected at high concentrations with a highly one-dimensional character. With magnetic colloids that form magnetic equilibrium structures according to cryo-TEM, it has been demonstrated that the response to an alternating field occurs at frequencies corresponding to the (slow) rotation of the dipolar structures.[26,27] This implies that measuring the dielectric response from rotation of individual particles is largely impeded because chains of different sizes have different relaxation times that are much longer than for single particles. Moreover, because particle concentrations have to be high enough to measure significant

signals, the number of single dipolar colloids present in the dispersion is limited, as the cluster size strongly depends on the concentration (see eq 2). It is, therefore, questionable whether methods based on the dielectric response from rotation of single particles are suitable to determine the dipole moment of colloidal nanocrystals when dipolar structures are involved. In contrast, the cryo-TEM analysis we presented here provides direct quantitative information on the pair interaction and equilibrium structures of nanocrystals in dispersion.

The presence of significant amounts of surface charge has a strong effect on the electronic properties of the nanocrystals. The pair interactions we determined correspond to a potential drop of several tens of a volt over the nanocrystals. Such a potential drop will distort the electronic wave functions and is likely to lift the degeneracy of all levels that are not spherically symmetric, leading to, e.g., broadening of excitonic transitions.

In conclusion, we have shown with in situ cryo-TEM that, in dispersions of PbSe and CdSe quantum dots, dipolar equilibrium structures form whose size mainly depends on concentration. Analyzing the cluster-size distribution with a one-dimensional aggregation model (eq 2) yields a pair attraction on the order of $8-10$ k_BT. Two-dimensional and 3D self-assembled structures of these NCs clearly indicate local crystallographic alignment between the colloids as a result of the dipolar coupling. These results are important for all measurements on relatively concentrated dispersions of nanocrystals because the distribution of chain lengths can influence the response of the system to optical and electrical signals. For example, efficient energy-transfer may occur within clusters. Understanding the chain formation and the distribution of chain lengths is also important for the synthesis of anisotropic nanocrystals such as wires, stars, and rings. This information may help in the design of novel functional nanomaterials.

References

(1) Tang, Z.; Kotov, N.; Giersig, M. *Science* **2002**, *297*, 237−240.

(2) Talapin, D. V.; Murray, C. B. *Science* **2005**, *310*, 86.

(3) Cho, K. S.; Talapin, D. V.; Gaschler, W.; Murray, C. B. *J. Am. Chem. Soc.* **2005**, *127*, 7140.

(4) Houtepen, A. J.; Koole, R.; Vanmaekelbergh, D. L.; Meeldijk, J.; Hickey, S. G. *J. Am. Chem. Soc.* **2006**, *128*, 6792.

(5) Blanton, S. A.; Leheny, R. L.; Hines, M. A.; Guyot-Sionnest, P. *Phys. Rev. Lett.* **1997**, *79*, 865.

(6) Li, L.; Alivisatos, A. *Phys. Rev. Lett.* **2003**, *90*, 097402.

(7) Shim, M.; Guyot-Sionnest, P. *J. Chem. Phys.* **1999**, *111*, 6955.

(8) Tang, Z.; Zhang, Z.; Wang, Y.; Glotzer, S.; Kotov, N. *Science* **2006**, *314*, 274.

(9) Talapin, D.; Shevchenko, V.; Murray, C. B.; Titov, A.; Král, P. *Nano Lett.* **2007**, *7*, 1213.

(10) Sashchiuk, A.; Amirav, L.; Bashouti, M.; Krueger, M.; Sivan, U.; Lifshitz, E. *Nano Lett.* **2004**, *4*, 159.

(11) Frederik, P. M.; Bomans, P. H. H.; Laeven, P. F. J.; Nijpels, F. J. T. *Device for Preparing Specimens for a Cryo-electron Microscope*; Netherlands Industrial Property Office (RO/NL) PCT/NL02/00189, 2002.

(12) Frederik, P. M.; Sommerdijk, N. *Curr. Opin. Colloid Interface Sci.* **2005**, *10*, 245.

(13) Butter, K.; Bomans, P. H. H.; Frederik, P. M.; Vroege, G. J.; Philipse, A. P. *Nat. Mater.* **2003**, *2*, 88.

(14) Klokkenburg, M.; Vonk, C.; Claesson, E. M.; Meeldijk, J. D.; Erné, B. H.; Philipse, A. P. *J. Am. Chem. Soc.* **2004**, *126*, 16706.

(15) Klokkenburg, M.; Erné, B. H.; Philipse, A. P. *Langmuir* **2005**, *21*, 1187.

(16) Klokkenburg, M.; Erné, B. H.; Meeldijk, J. D.; Wiedenmann, A.; Petukhov, A. V.; Dullens, R. P. A.; Philipse, A. P. *Phys. Rev. Lett.* **2006**, *97*, 185702.

(17) de Mello Donega, C.; Hickey, S.; Wuister, S.; Vanmaekelbergh, D.; Meijerink, A. *J. Phys. Chem. B* **2003**, *107*, 489.

(18) Butter, K.; Bomans, P. H.; Frederik, P. M.; Vroege, G. J.; Philipse, A. P. *J. Phys.: Condens. Matter* **2003**, *15*, S1451.

(19) Crocker, J. C.; Grier, D. G. *J. Colloid Interface Sci.* **1996**, *179*, 298.

(20) Younge, K.; Christenson, C.; Bohara, A.; Crnkovic, J.; Saulnier, P. *Am. J. Phys.* **2004**, *72*, 1247.

(21) Klokkenburg, M.; Dullens, R. P. A.; Kegel, W. K.; Erné, B. H.; Philipse, A. P. *Phys. Rev. Lett.* **2006**, *96*, 037203.

(22) Israelachvilli, J. *Intermolecular and Surface Forces*; Academic Press: San Diego, 1992; pp 341−360.

(23) Reiss, H.; Kegel, W. K.; Groenewold, J. *Ber. Bunsen-Ges. Phys. Chem.* **1996**, *100*, 279.

(24) Pietryga, J. M.; Schaller, R. D.; Werder, D.; Stewart, M. H.; Klimov, V. I.; Hollingsworth, J. A. *J. Am. Chem. Soc.* **2004**, *126*, 11752.

(25) In addition to its permanent dipole component, the NC may carry an additional contribution that results from the polarization of the NC by the strong fields caused by its neighbors. Depending on the exact charge distribution, we estimate the induced dipole to be 30 to 50 D for the 6.8 nm PbSe NCs. This value is an order of magnitude lower than the total dipole moment, which is, thus, dominated by the permanent component.

(26) Erné, B. H.; Butter, K.; Kuipers, B. W. M.; Vroege, G. J. *Langmuir* **2003**, *19*, 8218.

(27) Klokkenburg, M.; Erné, B. H. *J. Magn. Magn. Mater.* **2006**, *306*, 85.

NL0714684